Hindawi
Advances in Materials Science and Engineering
Volume 2017, Article ID 6123628, 8 pages
https://doi.org/10.1155/2017/6123628

Research Article

Electrical and Vibrational Studies of $Na_2K_2Cu(MoO_4)_3$

Wassim Dridi,[1] Mohamed Faouzi Zid,[1] and Miroslaw Maczka[2]

[1]*Laboratory of Materials, Crystal Chemistry and Applied Thermodynamics, Faculty of Sciences of Tunis, University of Tunis El Manar, El Manar II, 2092 Tunis, Tunisia*
[2]*Institute of Low Temperature and Structure Research, Polish Academy of Sciences, P.O. Box 1410, 50-950 Wrocław 2, Poland*

Correspondence should be addressed to Mohamed Faouzi Zid; faouzi.zid@fst.rnu.tn

Received 1 December 2016; Revised 6 March 2017; Accepted 27 March 2017; Published 11 June 2017

Academic Editor: Pascal Roussel

The complex impedance of $Na_2K_2Cu(MoO_4)_3$ material has been investigated in the temperature range of 653–753 K and in the frequency range of 40 Hz–5 MHz. Electrical behavior of the studied material is explained through an equivalent circuit model which takes into account the contributions of grains and grains boundaries. The number of vibrational modes was calculated using group theoretical approach. The infrared and Raman spectra have also been measured and vibrational assignment has been proposed.

1. Introduction

A great deal of interest has been devoted to the chemistry of molybdenum; a significant number of new molybdates have been synthesized and characterized. Molybdate chemistry has developed rapidly and this development can be explained by several factors, especially the improvement of the structural X-ray diffraction analysis, which has been a fundamental tool used for determination of crystal structures. But this renewed interest is also explained by the fact that many molybdates are suitable materials for technological applications. Molybdates exhibit various physicochemical properties, which are related to both the nature of the elements associated with the molybdate groups and the degree of opening of the formed framework. In these materials, the anionic framework is usually built from MoO_4 tetrahedra linked to the transition metal polyhedra, leading to a large variety of crystal structures with a high capacity for cationic substitution. The chemistry of inorganic molybdate materials has been significantly advanced thanks to their valuable electrical and optical properties, which make them promising for various applications such as photoluminescence [1], ionic conductivity [2–4], laser materials [5, 6], and piezoelectrics [7]. The high-temperature superconductivity present in the copper-oxygen ceramic systems resulted in an increasing structural and physicochemistry interest of materials containing Cu-O [8]. Among these materials we can mention the copper molybdate $Cu_3Mo_2O_9$ doped with lithium, which displays high coulombic efficiency in lithium-ion batteries and excellent charge-discharge stability [9]. Another example is $Li_2Cu_2(MoO_4)_3$ material, which presents a high ionic conductivity ($\sigma = 5.810^{-3}$ $Ohm^{-1}\cdot cm^{-1}$ at 400 K, $E_a = 0.33$ eV) [10].

The vibrational spectroscopic studies of molybdates have attracted particular attention of a large number of researchers [11–16]. This attention is due to the catalytic activity of (MoO_4^{2-}) groups in hydrocarbons oxidations [17–20] and due to negative thermal expansion, ferroelasticity, and pressure-induced amorphization [21]. Furthermore, the interpretation of laser properties needs knowledge of vibrational level distribution [22]. According to this approach, we have decided to explore system A-Mo-Cu-O (A = alkali metal). The purpose of this study is to analyze the electrical response of the grain and grains boundaries effects, which greatly influence the electrical properties, and to understand the molecular structure at microscopic level of novel $Na_2K_2Cu(MoO_4)_3$ compound. This study can provide important information on the conductivity, which is very important for practical applications. In this paper, we will describe the synthesis method and the characterization of $Na_2K_2Cu(MoO_4)_3$ by Infrared, Raman, and complex impedance spectroscopies. Raman and IR selection rules will be also analyzed using factor group analysis.

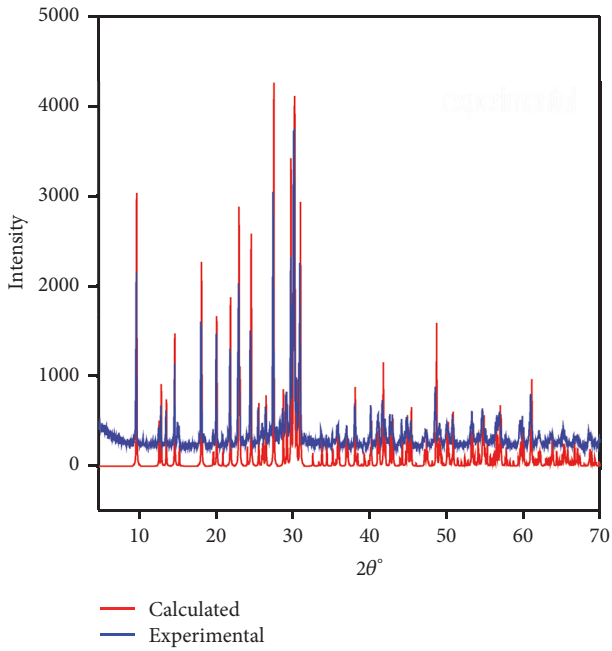

Figure 1: Calculated and experimental powder X-ray diffraction patterns of $Na_2K_2Cu(MoO_4)_3$.

2. Experimental

2.1. Polycrystalline Powder Synthesis of $Na_2K_2Cu(MoO_4)_3$. The $Na_2K_2Cu(MoO_4)_3$ polycrystalline powder was prepared by a conventional solid-state reaction from high-purity starting reagents of Na_2CO_3, K_2CO_3, $Cu(CO_2CH_3)\cdot H_2O$, and $(NH_4)_6Mo_7O_{24}\cdot 4H_2O$. These reagents were weighted according to the stoichiometric ratio. They were mixed and ground together in an agate mortar and heated progressively to 773 K in porcelain crucible with intermittent cooling and regrindings. The powder was analyzed by X-ray powder diffraction, using a PAN-analytical X'Pert PRO X-ray diffractometer equipped with copper anticathode (λK_α = 1.5406 Å). The unit cell parameters were refined using Celref 3.0 program and calculated to be as follows: a = 7.5010(7) Å, b = 9.3411(4) Å, and c = 9.3670(7) Å and α = 92.59(3)°, β = 105.32(9)°, and γ = 105.44(6)°. The powder X-ray diffraction pattern was in agreement with single-crystal structure (Figure 1).

2.2. Complex Impedance Spectroscopy. Pellet was prepared by isostatic pressing at 4 kbar and sintering at 773 K for 12 h in air with 10 $Kmin^{-1}$ heating and cooling rates. The thickness and surface of pellet were about 0.22 cm and 1.25 cm^2 having a geometric factor of $e/s = 0.176$ cm^{-1}. Electrical measurements were carried out in air by complex impedance spectroscopy using Agilent 4294A Precision Impedance Analyzer in the 40 Hz–5 MHz frequency range and 653–753 K temperature range. The sinusoidal AC voltage applied is of 0.5 V. The measuring cell having the sample inserted between two platinum discs used as ion-blocking electrodes is heated in an electric oven under dry air. The measurements were carried out after temperature stabilization of the device every 30 min with a pitch of 10 K. The advantage of this method lies in the fact that it is possible to separate the physical phenomena according to their speed; the fast phenomena will take place at high frequencies and the slow ones at low frequencies. Analysis of impedance spectroscopy data can provide information on charge carrier dynamics in ionic conductors [23].

2.3. Vibrational Spectroscopies. The infrared spectrum was recorded at room temperature using Thermo Scientific Nicolet iS50 FT-IR Spectrometer. The frequency range was from 400 to 4000 cm^{-1} and the spectral resolution was 3 cm^{-1}. We are interested only in the domain 400–1100 cm^{-1} containing the most significant solid-state absorption bands. To obtain the Raman spectrum of the powdered sample, LAB RAMAN HR800 spectrometer was used. The frequency range was from 100 to 1100 cm^{-1} and the spectral resolution was 2 cm^{-1}. The measurement was carried out on a thin pellet. The sample was analyzed with an excitation wavelength of 632.81 nm and a power was adjusted to 1 mW in order to avoid any degradation. Spectroscopic studies are used to obtain the distribution of vibrational levels and assignment to the respective normal modes of $Na_2K_2Cu(MoO_4)_3$.

3. Results and Discussion

3.1. Structure Description. $Na_2K_2Cu(MoO_4)_3$ crystallizes in the triclinic space group P-1 with a = 7.4946(8) Å, b = 9.3428(9) Å, c = 9.3619(9) Å, α = 92.591(7)°, β = 105.247(9)°, γ = 105.496(9)°, V = 604.7(Å^3), Z = 2, $R(F^2)$ = 0.022, and $R_w(F^2)$ = 0.056. Both cations K1 and K3 are located in the center of inversion, and all other atoms are at general positions. The structure of $Na_2K_2Cu(MoO_4)_3$ can be described as a one-dimensional framework formed by ribbons arranged in parallel to a axis with interribbons spaces containing Na^+ and K^+ monovalent cations directed to the free vertices of the tetrahedra MoO_4 (Figure 2). These structural characteristics encouraged us to study the electrical properties. CIF file containing complete information on the studied structure was deposited with FIZ Karlsruhe, 76344 Eggenstein-Leopoldshafen, Germany (fax: (+49)7247-808-666; e-mail: crysdata(at)fiz-karlsruhe(dot)de, deposition number CSD-430379).

3.2. Electrical Properties. The Nyquist plots in the temperature range from 653 K to 753 K are shown in Figure 3. When temperature increases, the radius of semicircles decreases and consequently the ionic conductivities increase with the temperature. We notice the presence of two hardly distinguishable semicircles, which proves the presence of two relaxation phenomena. The first arc existing towards higher frequencies corresponds to the movement of ions across the grain (bulk), which represents intrinsic conduction and gives rise to an intragranular resistance. The second arc, observed at lower-frequency, corresponds to movement of ions through the grain boundaries [24, 25]. The electrical behavior of $Na_2K_2Cu(MoO_4)_3$ is interpreted through an equivalent electrical circuit formed by two cells arranged

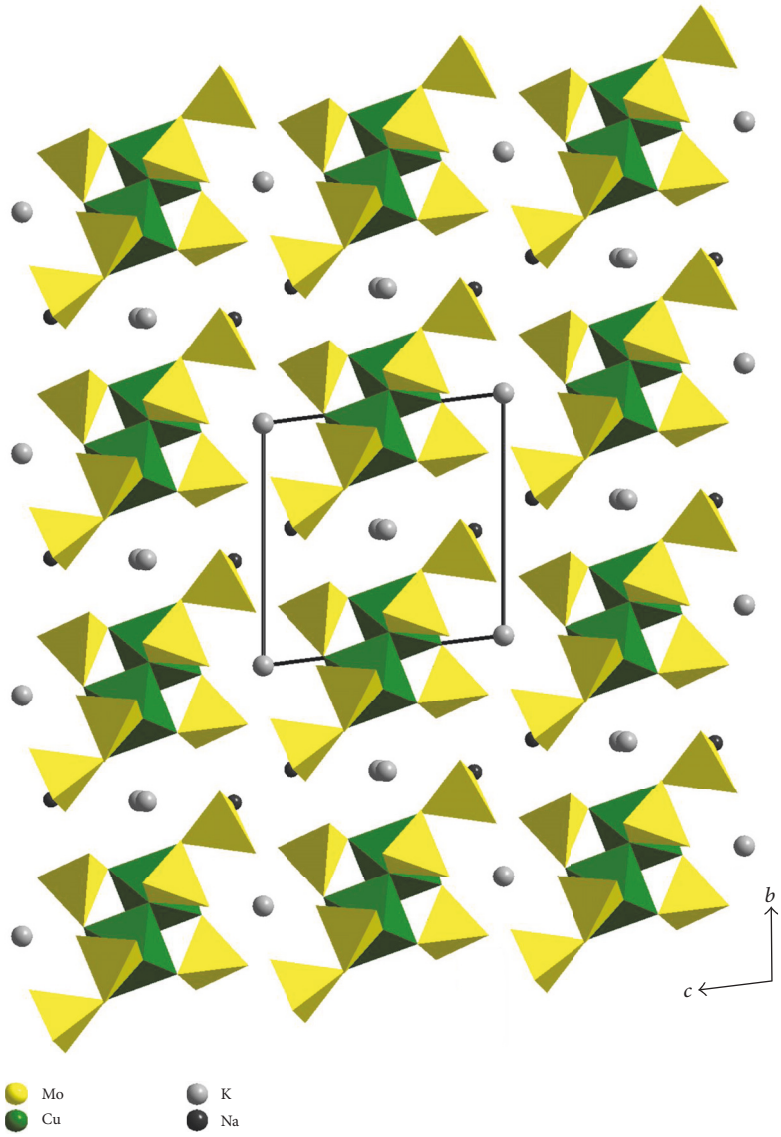

FIGURE 2: Projection of $Na_2K_2Cu(MoO_4)_3$ structure according to *a* axis.

in series, constituted by the parallel combination of the following: $R_g \parallel C1$ and $R_{gb} \parallel$ CPE1 corresponding to the contributions of grains and grains boundaries, respectively. R_g and R_{gb} are the resistances of grains and grains boundaries, respectively. C1 is the pure capacitance of grain and CPE1 is the fractal capacitance constant phase element according to grains boundary. Electrical parameters were measured as a function of temperature. The intercepts of the semicircular arcs with the real axis give an estimation of the resistance of the studied material. Zview software [26] was used to fit these curves. The total resistance, R_{total}, follows the relation $R_g + R_{gb} = R_{total}$. The conformity between the experimental and calculated curves (fit) on the whole temperature range proves the validity of the proposed equivalent circuit. Electrical parameters are represented in Table 1.

In order to determine the direct conductivity for the grain interior σ_g, grain boundary σ_{gb}, and total conductivity σ_{tot}, we used the following equation:

$$\sigma_i = \frac{e}{R_i} \cdot \frac{1}{s}. \quad (1)$$

Values of ionic conductivities in $Na_2K_2Cu(MoO_4)_3$ material are represented in Table 2.

The activation energies was obtained by linear fitting of the ionic conductivities values at different temperatures by applying the Arrhenius equation:

$$T = \sigma_0 \exp\left(-\frac{E_a}{k_b T}\right), \quad (2)$$

where σ is the temperature dependent ionic conductivity, σ_0 is the ionic conductivity at absolute zero temperature,

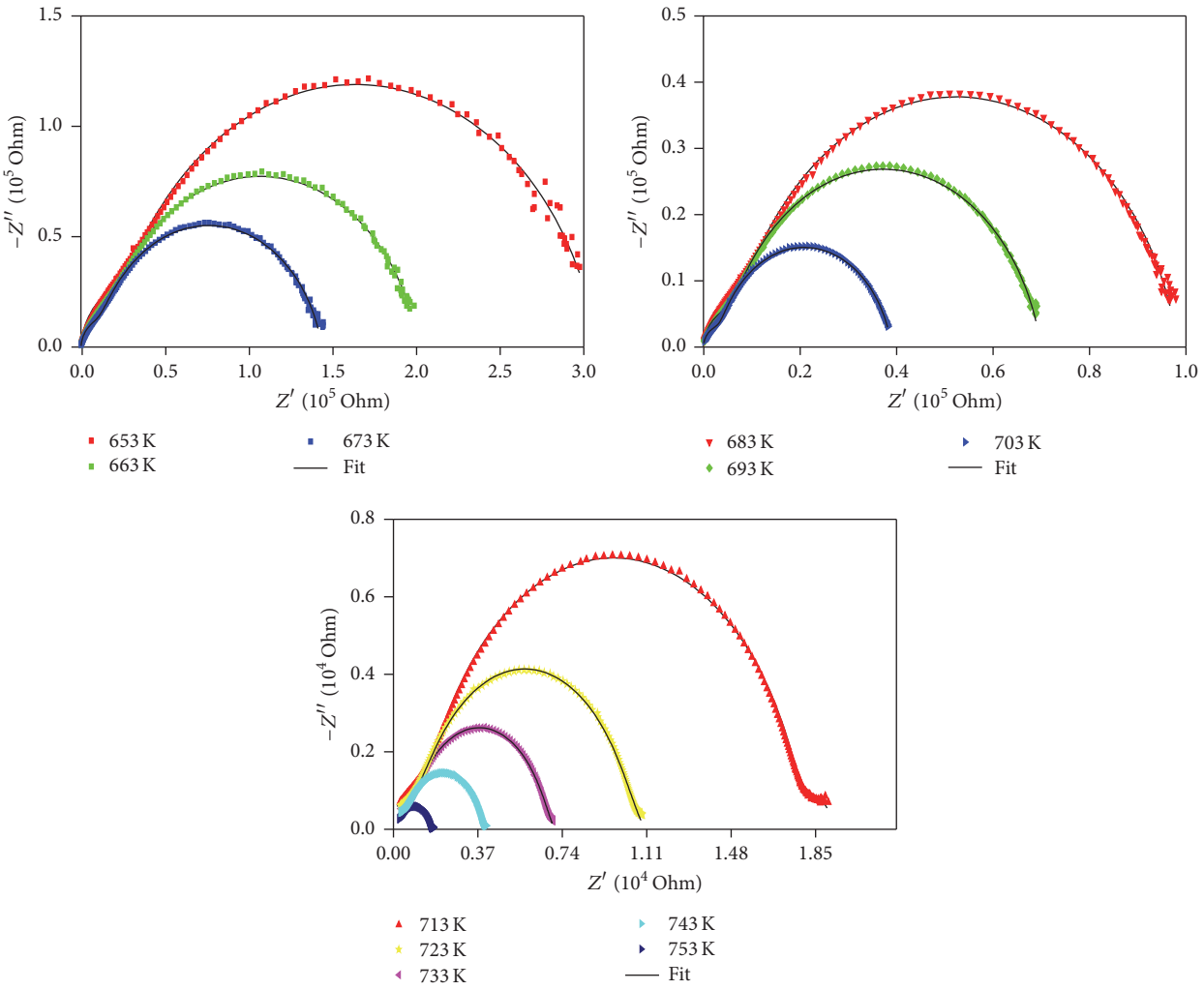

Figure 3: Complex impedance spectrum of $Na_2K_2Cu(MoO_4)_3$ over temperature range 653 and 753 K.

Table 1: Simulated data of the electrical parameters for the proposed equivalent circuit.

T (K)	R_g (Ω)	C_g (F)	R_{gb} (Ω)	C_{gb} (F)	$\sum R_i$ (Ω)
653	$2.087(4)10^5$	$1.118(2)10^{-11}$	$2.874(1)10^6$	$8.683(2)10^{-11}$	$3.083(1)10^6$
663	$1.354(1)10^5$	$1.078(1)10^{-11}$	$1.877(2)10^6$	$9.442(1)10^{-11}$	$2.012(2)10^6$
673	$9.711(9)10^4$	$9.131(4)10^{-11}$	$1.339(2)10^6$	$9.908(4)10^{-11}$	$1.436(2)10^6$
683	$6.797(9)10^4$	$9.639(5)10^{-12}$	$9.159(1)10^5$	$1.032(1)10^{-10}$	$9.838(9)10^5$
693	$4.915(3)10^4$	$9.010(1)10^{-12}$	$6.499(8)10^5$	$1.078(3)10^{-10}$	$6.991(3)10^5$
703	$2.913(9)10^4$	$7.893(2)10^{-12}$	$3.610(6)10^5$	$1.145(4)10^{-10}$	$3.901(9)10^5$
713	$1.283(3)10^4$	$6.905(2)10^{-12}$	$1.677(1)10^5$	$1.349(2)10^{-10}$	$1.805(3)10^5$
723	$8.670(1)10^3$	$6.781(3)10^{-12}$	$9.794(8)10^4$	$1.518(1)10^{-10}$	$1.066(1)10^5$
733	$6.670(2)10^3$	$6.793(4)10^{-12}$	$6.197(5)10^4$	$1.578(2)10^{-10}$	$6.864(5)10^4$
743	$4.831(3)10^3$	$7.066(1)10^{-12}$	$3.464(6)10^4$	$1.803(2)10^{-10}$	$3.947(7)10^4$
753	$2.715(2)10^3$	$7.954(2)10^{-12}$	$1.377(1)10^4$	$1.984(2)10^{-10}$	$1.648(6)10^4$

E_a is the activation energy of cations migration, k_b is the Boltzmann constant, and T is the absolute temperature. The variation of $\log(\sigma(S{\cdot}K{\cdot}cm^{-1}))$ versus $1000/T$ (K^{-1}) is represented in Figure 4. Activation energies values are represented in Table 3.

We note that the total conductivity of our compound is less than the bulk conductivity but higher than the grain boundary one. This reveals the existence of a partial blockage of the charge carriers by the grain boundaries [27]. Therefore, the conductivity of our material is limited by the

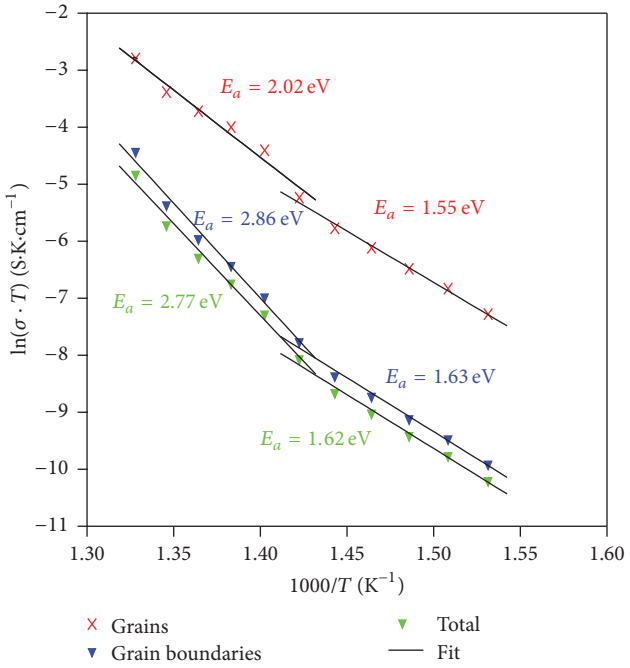

Figure 4: Arrhenius plot of conductivity of $Na_2K_2Cu(MoO_4)_3$.

Table 2: Ionic conductivities measurements value as a function of temperature in $Na_2K_2Cu(MoO_4)_3$ material.

T (K)	Conductivities (Ω cm^{-1})		
	σ_g	σ_{gb}	σ_{total}
653	1.05310^{-6}	7.65210^{-8}	5.70710^{-8}
663	1.62410^{-6}	1.17210^{-7}	8.74510^{-8}
673	2.26510^{-6}	1.64210^{-7}	1.22510^{-7}
683	3.23610^{-6}	2.40110^{-7}	1.78810^{-7}
693	4.47510^{-6}	3.38410^{-7}	2.51710^{-7}
703	7.55010^{-6}	6.09310^{-7}	4.51010^{-7}
713	1.71410^{-5}	1.31110^{-6}	9.74810^{-7}
723	2.53710^{-5}	2.24610^{-6}	1.65010^{-6}
733	3.29810^{-5}	3.54910^{-6}	2.56310^{-6}
743	4.55310^{-5}	6.34910^{-6}	4.45810^{-6}
753	8.10310^{-5}	1.59710^{-5}	1.06710^{-5}

low conductivity of the grain boundaries. The influence of the grains boundaries conductivity on the total conductivity can be evaluated quantitatively by the blocking factor α. This parameter characterizes the fraction of the load carriers blocked in the case where a direct current flows through the sample. It can also be calculated using the following equation [28, 29]:

$$\alpha = \frac{R_{gb}}{R_{tot}}. \quad (3)$$

Figure 5 shows the variation of the blocking factor as a function of the temperature. It is found that the blocking factor decreases with the temperature. Therefore, the increase in temperature causes a decrease in the blocking effect by the limits of the grains.

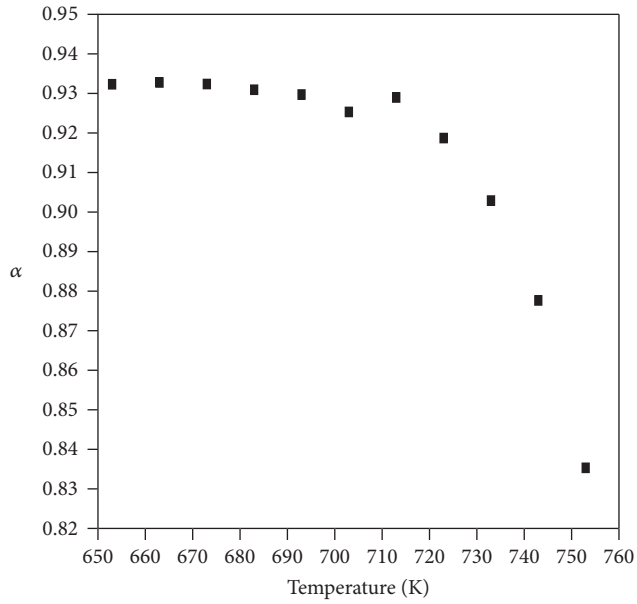

Figure 5: Variation of the blockage factor α with temperature.

Table 3: Activation energies in $Na_2K_2Cu(MoO_4)_3$ material.

Contribution	Temperature range (K)	E_a (eV)
Grains	653–673	1.55
	673–753	2.02
Grains boundaries	653–673	1.63
	673–753	2.86
Total	653–673	1.62
	673–753	2.77

3.3. Vibrational Study. $Na_2K_2Cu(MoO_4)_3$ crystallizes in the triclinic space group P-1 which corresponds to C_i factor group. There are two molecules per unit-cell, so there are also two molecules per Bravais cell. Mo1, Mo2, Mo3, Cu1, K2, Na1, Na1, and O atoms occupy C_1 symmetry whereas K1 and K3 atoms occupy C_i symmetry. The Bravais cell comprises 40 atoms that have 120 zone center degrees of freedom. The structure of $Na_2K_2Cu(MoO_4)_3$ compound is centrosymmetric; a complete assignment of the crystal modes requires both IR and Raman spectra [30]. The crystal vibrational modes are obtained by group theoretical calculations developed by Fateley et al. [31]. Factor group analysis of $Na_2K_2Cu(MoO_4)_3$ is represented in Table 4. The vibrational irreducible representation for the triclinic phase at the center of the Brillouin zone ($k = 0$) is

$$\Gamma_{vibr} = 57A_g + 63A_u, \quad (4)$$

3 acoustic and $(3N - 3)$ optic modes, where N is the number of atoms in the unit cell [32]:

$$\Gamma_{acoustic} = 3A_u$$
$$\Gamma_{optic} = 57A_g + 60A_u. \quad (5)$$

Table 4: Factor group analysis of the triclinic phase $Na_2K_2Cu(MoO_4)_3$.

	Atoms	Site symmetry	n_s	t_γ	γ	f_γ	ζ	C_ζ	a_ζ	$\sum \Gamma_{atom}$
P-1	Γ_{transl} Mo1, Mo2, Mo3, Cu1, K2, Na1, Na2, 12 O	C_1	2	3	$A(T_x, T_y, T_z)$	6	A_g	1	3	$19(3A_g + 3A_u)$
$Z = 2$							A_u	1	3	
$Z^B = 2$	Γ_{transl} K1, K3	C_i	1	3	$A_u(T_x, T_y, T_z)$	3	A_u	1	3	$2(3A_u)$

Z^B: number of molecules per primitive Bravais cell, n_s: number of positions, t_γ: number of translations of a site species γ, and f_γ: the degree of vibrational freedom present in each site species γ.
C_ζ represents the degeneracy of the species ζ of the factor group, whereas a_ζ is the number of lattice vibrations of the equivalent set of atoms in species ζ of the factor group.

Infrared and Raman active modes are as follows:

$$\Gamma_{raman} = 57A_g$$
$$\Gamma_{infrared} = 60A_u. \quad (6)$$

In the free state tetrahedral MoO_4 ion has T_d symmetry and four vibrational modes with the following wavenumbers: $\nu_1(A_1)$ nondegenerate symmetric stretching at 936 cm^{-1}, $\nu_2(E)$ doubly degenerate symmetric bending at 220 cm^{-1}, $\nu_3(F_2)$ triply degenerate asymmetric stretching at 895 cm^{-1}, and $\nu_4(F_2)$ triply degenerate asymmetric bending at 365 cm^{-1} [33]. Moreover, all four vibrational modes are active in the Raman spectra, but only F_2 stretching and bending vibrations are active in the IR spectra. However, when this ion is located in the crystal lattice, its symmetry is lowered due to the constraints imposed by the lattice. So, the local symmetry of the three MoO_4 tetrahedra decreases to C_1. Because of this lowering of symmetry, all modes become active in Raman and in infrared and degenerate modes raise their degenerations. Therefore, ν_3 and ν_4 are split into three bands $3A$ and ν_2 into two $2A$. The correlation between the point group of T_d symmetry of the free anion MoO_4, its site-symmetry C_1, and its factor group C_i is represented in Scheme 1. According to Basiev et al. [34], the vibrational modes observed in Raman spectra of molybdates can be classified into two groups, internal and external modes. The internal vibrational modes of each type of MoO_4 derived from the correlation scheme are equal to $Z(3n - 6) = 18$, where n is the number of atoms in the molecular MoO_4:

$$\Gamma_{MoO_4} = 9A_g^{(R)} + 9A_u^{(IR)}$$
$$\Gamma\nu_1 = A_g^{(R)} + A_u^{(IR)}$$
$$\Gamma\nu_2 = 2A_g^{(R)} + 2A_u^{(IR)}$$
$$\Gamma\nu_3 = 3A_g^{(R)} + 3A_u^{(IR)}$$
$$\Gamma\nu_4 = 3A_g^{(R)} + 3A_u^{(IR)}. \quad (7)$$

The external vibrational modes of MoO_4 are divided into translational modes which includes acoustic and lattice modes and librational modes [35], presented as follows:

$$\Gamma_{translation} = \Gamma_{acoustic} + \Gamma_{lattice} = 3A_g^{(R)} + 3A_u^{(IR)}$$
$$\Gamma_{libration} = 3A_g^{(R)} + 3A_u^{(IR)}. \quad (8)$$

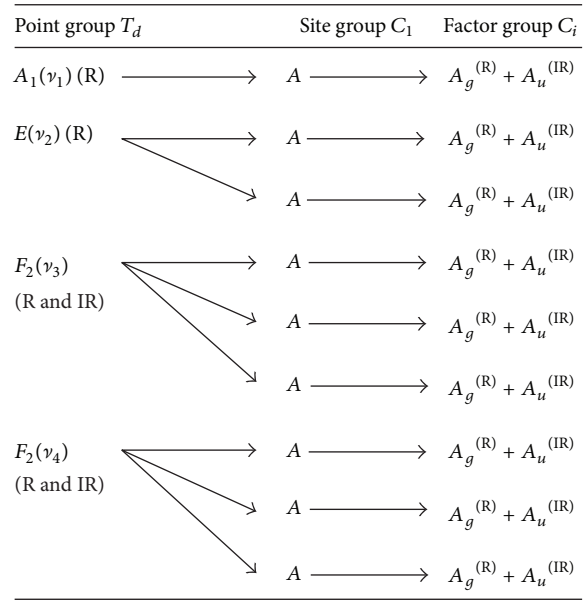

Scheme 1: Correlation scheme for the internal modes of MoO_4 in $Na_2K_2Cu(MoO_4)_3$ structure.

The comparison of the infrared and Raman bands positions shows that the majority of these bands do not coincide. Indeed, the observed IR bands appear at wavenumbers different from those in the Raman spectrum (Figure 6). This is in agreement with the centrosymmetric character of $Na_2K_2Cu(MoO_4)_3$ structure [36]. The Raman spectrum can be separated into two parts with a wide empty gap in the range 500–700 cm^{-1} that is commonly observed in molybdates containing MoO_4 tetrahedra [22, 37–43]. The proposed assignment of the vibrational spectra of MoO_4 in $Na_2K_2Cu(MoO_4)_3$ is realised by considering the following criteria: ν_1 bands are generally very strong in the Raman and weaker in the infrared spectra, whereas an opposite behavior is usually observed for ν_3 bands. ν_2 bands are usually stronger in the Raman spectra than those corresponding to ν_4 modes but in the infrared spectra ν_4 band is generally more intense [44]. The Mo-O stretching modes are located in the range 720–930 cm^{-1} whereas the bending modes are situated in the range 380–330 cm^{-1}. Wavenumbers and assignment of the internal vibrational modes of MoO_4 tetrahedron are listed in Table 5.

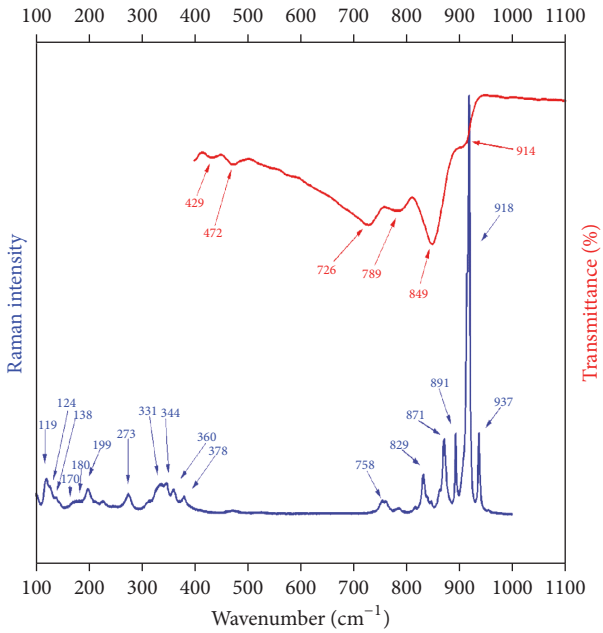

Figure 6: Infrared and Raman spectra of $Na_2K_2Cu(MoO_4)_3$.

Table 5: Assignment of the internal vibrational modes frequencies of MoO_4 tetrahedron.

Assignment	Infrared (ν/cm^{-1})	Raman (ν/cm^{-1})
$\nu_1(MoO_4)$	914	937, 918, 891
$\nu_2(MoO_4)$		344, 331, 273
$\nu_3(MoO_4)$	849, 789, 726	871, 829, 758
$\nu_4(MoO_4)$	429, 472	378, 360

In the Raman spectrum, bands located below 300 cm^{-1} are attributed to external vibrations involving the librational and translational modes of the MoO_4 anions and translational modes of cations; the distinguishing between librational and translational modes is difficult. But in general librational modes have higher wavenumbers and intensities than the translational modes [45]. Furthermore, since the atomic mass of molybdenum is larger than that of copper, potassium, and sodium, translations of the MoO_4^{-2} ions should be observed at lower wavenumbers than translations of Cu^{2+}, K^+, and Na^+ [13]. Based on these rules, we propose assignment of the 273 cm^{-1} band to $T'(Na^+)$ modes, those at 119 and 124 cm^{-1} to $L(MoO_4)$ modes, and the remaining bands in the 138–199 cm^{-1} range to the coupled modes involving translational motions of the molybdate, potassium, and copper ions.

4. Conclusion

Polycrystalline powder of $Na_2K_2Cu(MoO_4)_3$ was obtained by standard solid-state reaction at 773 K. X-ray diffraction studies show that this compound crystallizes in the triclinic symmetry with the P-1 space group. Ionic conductivity of the investigated material is characterized by the existence of a partial blockage of the charge carriers by the grain boundaries. The blocking effect generated by the limits of the grains decreases with temperature. The centrosymmetric space group P-1 of our structure is confirmed by the noncoincidence of majority of Raman and IR bands. Vibrational study indicates the lowering of symmetry of molybdate anion from T_d to C_1 symmetry.

Conflicts of Interest

The authors declare that there are no conflicts of interest regarding the publication of this paper.

References

[1] R. Grasser, E. Pitt, A. Scharmann, and G. Zimmerer, "Optical properties of $CaWO_4$ and $CaMoO_4$ crystals in the 4 to 25 eV region," *physica Status Solidi (b)*, vol. 69, no. 2, pp. 359–368, 1975.

[2] A. A. Savina, S. F. Solodovnikov, D. A. Belov et al., "Synthesis, crystal structure and properties of alluaudite-like triple molybdate $Na_{25}Cs_8Fe_5(MoO_4)_{24}$," *Journal of Solid State Chemistry*, vol. 220, pp. 217–220, 2014.

[3] M. Hartmanova, M. T. Le, M. Jergel, V. Šmatko, and F. Kundracik, "Structure and electrical conductivity of multicomponent metal oxides having scheelite structure," *Russian Journal of Electrochemistry*, vol. 45, no. 6, pp. 621–629, 2009.

[4] N. I. Sorokin, "Ionic conductivity of double sodium-scandium and cesium-zirconium molybdates," *Physics of the Solid State*, vol. 51, no. 6, pp. 1128–1130, 2009.

[5] Y. Zhang, H. Cong, H. Jiang, J. Li, and J. Wang, "Flux growth, structure, and physical characterization of new disordered laser crystal $LiNd(MoO_4)_2$," *Journal of Crystal Growth*, vol. 423, pp. 1–8, 2015.

[6] N. M. Kozhevnikova and O. A. Kopylova, "Synthesis and X-ray diffraction and IR spectroscopy studies of ternary molybdates $Li_3Ba_2R_3(MoO_4)_8$ (R = La-Lu, Y)," *Russian Journal of Inorganic Chemistry*, vol. 56, no. 6, pp. 935–938, 2011.

[7] A. E. Sarapulova, B. Bazarov, T. Namsaraeva et al., "Possible piezoelectric materials $CsMZr_{0.5}(MoO_4)_3$ (M = Al, Sc, V, Cr, Fe, Ga, In) and $CsCrTi_{0.5}(MoO_4)_3$: structure and physical properties," *Journal of Physical Chemistry C*, vol. 118, no. 4, pp. 1763–1773, 2014.

[8] J. Hanuza, M. Andruszkiewicz, Z. Bukowski, R. Horyń, and J. Klamut, "Vibrational spectra and internal phonon calculations for the $M_2Cu_2O_5$ binary oxides (M = In, Sc, Y or from Tb to Lu)," *Spectrochimica Acta Part A: Molecular Spectroscopy*, vol. 46, no. 5, pp. 691–704, 1990.

[9] J. Xia, L. X. Song, W. Liu et al., "Highly monodisperse $Cu_3Mo_2O_9$ micropompons with excellent performance in photocatalysis, photocurrent response and lithium storage," *RSC Advances*, vol. 5, no. 16, pp. 12015–12024, 2015.

[10] S. F. Solodovnikov, R. F. Klevtsova, and P. V. Klevtsov, "A correlation between the structure and some physical properties of binary molybdates (Tungstates) of uni- and bivalent metals," *Journal of Structural Chemistry*, vol. 35, no. 6, pp. 879–889, 1994.

[11] S. S. Saleem, G. Aruldhas, and H. D. Bist, "Raman and infrared spectra of GdTb $(MoO_4)_3$ single crystal in the region 250–1000 cm-1," *Spectrochimica Acta Part A: Molecular Spectroscopy*, vol. 39, no. 12, pp. 1049–1053, 1983.

[12] B. G. Bazarov, R. F. Klevtsova, T. T. Bazarova et al., "Double molybdate $Tl_2Mg_4(MoO_4)_3$: synthesis, structure, and properties," *Russian Journal of Inorganic Chemistry*, vol. 51, no. 10, pp. 1577–1580, 2006.

[13] M. MacZka, A. Pietraszko, W. Paraguassu et al., "Structural and vibrational properties of $K_3Fe(MoO_4)_2(Mo_2O_7)$—a novel layered molybdate," *Journal of Physics Condensed Matter*, vol. 21, no. 9, Article ID 095402, 2009.

[14] M. Isaac, V. U. Nayar, D. D. Makitova, V. V. Tkachev, and L. O. Atovmjan, "Infrared and polarized Raman spectra of $LiNa_3(MoO_4)_2 \cdot 6H_2O$," *Spectrochimica Acta. Part A: Molecular and Biomolecular Spectroscopy*, vol. 53, no. 5, pp. 685–691, 1997.

[15] N. M. Kozhevnikova, "Synthesis and phase formation study in K_2MoO_4-$SrMoO_4$-$R_2(MoO_4)_3$ systems (where R = Pr, Nd, Sm, Eu, and Gd)," *Russian Journal of Inorganic Chemistry*, vol. 57, no. 5, pp. 646–649, 2012.

[16] R. L. Frost, J. Bouzaid, and I. S. Butler, "Raman spectroscopic study of the molybdate mineral Szenicsite and comparison with other paragenetically related molybdate minerals," *Spectroscopy Letters*, vol. 40, no. 4, pp. 603–614, 2007.

[17] S. S. Saleem, "Infrared and Raman spectroscopic studies of the polymorphic forms of nickel, cobalt and ferric molybdates," *Infrared Physics*, vol. 27, no. 5, pp. 309–315, 1987.

[18] Y. S. Yoon, W. Ueda, and Y. Moro-oka, "Selective conversion of propane to propene by the catalytic oxidative dehydrogenation over cobalt and magnesium molybdates," *Topics in Catalysis*, vol. 3, no. 3-4, pp. 265–275, 1996.

[19] W. Ueda, Y.-S. Yoon, K.-H. Lee, and Y. Moro-oka, "Catalytic oxidation of propane over molybdenum-based mixed oxides," *Korean Journal of Chemical Engineering*, vol. 14, no. 6, pp. 474–478, 1997.

[20] J. D. Pless, B. B. Bardin, H.-S. Kim et al., "Catalytic oxidative dehydrogenation of propane over Mg-V/Mo oxides," *Journal of Catalysis*, vol. 223, no. 2, pp. 419–431, 2004.

[21] M. MacZka, A. G. Souza Filho, W. Paraguassu, P. T. C. Freire, J. Mendes Filho, and J. Hanuza, "Pressure-induced structural phase transitions and amorphization in selected molybdates and tungstates," *Progress in Materials Science*, vol. 57, no. 7, pp. 1335–1381, 2012.

[22] J. Hanuza and L. Macalik, "Polarized i.r. and Raman spectra of orthorhombic $KLn(MoO_4)_2$ crystals (Ln = Y, Dy, Ho, Er, Tm, Yb, Lu)," *Spectrochimica Acta Part A: Molecular Spectroscopy*, vol. 38, no. 1, pp. 61–72, 1982.

[23] A. Lasia, *Electrochemical Impedance Spectroscopy and Its Applications*, vol. 32 of *Modern Aspects of Electrochemistry*, Springer US, 2002.

[24] B. Louati and K. Guidara, "Dielectric relaxation and ionic conductivity studies of $LiCaPO_4$," *Ionics*, vol. 17, no. 7, pp. 633–640, 2011.

[25] H. Mahamoud, B. Louati, F. Hlel, and K. Guidara, "Impedance and modulus analysis of the $(Na_{0.6}Ag_{0.4})_2PbP_2O_7$ compound," *Journal of Alloys and Compounds*, vol. 509, no. 20, pp. 6083–6089, 2011.

[26] D. Johnson, *Zview Version 3.1c*, Scribner Associates, 1990–2007.

[27] R. Ben Said, B. Louati, and K. Guidara, "Conductivity behavior of the new pyrophosphate $NaNi_{1.5}P_2O_7$," *Ionics*, vol. 22, no. 2, pp. 241–249, 2016.

[28] R. Gerhardt and A. S. Nowick, "Grain-boundary effect in ceria doped with trivalent cations: I, electrical measurements," *Journal of the American Ceramic Society*, vol. 69, no. 9, pp. 641–646, 1986.

[29] M. J. Verkerk, B. J. Middelhuis, and A. J. Burggraaf, "Effect of grain boundaries on the conductivity of high-purity ZrO_2—Y_2O_3 ceramics," *Solid State Ionics*, vol. 6, no. 2, pp. 159–170, 1982.

[30] J. Hanuza, "Raman scattering and infra-red spectra of tungstates $KLn(WO_4)_2$ family (Ln = La÷Lu)," *Journal of Molecular Structure*, vol. 114, pp. 471–474, 1984.

[31] W. G. Fateley, F. R. Dollish, N. J. McDevitt, and F. F. Bentley, *Infrared and Raman Selection Rules for Molecular and Lattice Vibrations: The Correlation Method*, John Wiley & Sons, New York, NY, USA, 1972.

[32] E. D. Palik, *Handbook of Optical Constants of Solids*, vol. 2, Academic Press, 1991.

[33] K. Nakamoto, *Infrared and Raman Spectra of Inorganic and Coordination Compounds*, Mir, Moscow, Russia, 1966.

[34] T. T. Basiev, A. A. Sobol, P. G. Zverev, L. I. Ivleva, V. V. Osiko, and R. C. Powell, "Raman spectroscopy of crystals for stimulated Raman scattering," *Optical Materials*, vol. 11, no. 4, pp. 307–314, 1999.

[35] L. Nalbandian and G. N. Papatheodorou, "Raman spectra and molecular vibrations of Au_2Cl_6 and $AuAlCl_6$," *Vibrational Spectroscopy*, vol. 4, no. 1, pp. 25–34, 1992.

[36] S. Kaoua, S. Krimi, S. Péchev et al., "Synthesis, crystal structure, and vibrational spectroscopic and UV-visible studies of $Cs_2MnP_2O_7$," *Journal of Solid State Chemistry*, vol. 198, pp. 379–385, 2013.

[37] J. Hanuza, L. Macalik, and K. Hermanowicz, "Vibrational properties of $KLn(MoO_4)_2$ crystals for light rare earth ions from lanthanum to terbium," *Journal of Molecular Structure*, vol. 319, pp. 17–30, 1994.

[38] V. V. Atuchin, O. D. Chimitova, T. A. Gavrilova et al., "Synthesis, structural and vibrational properties of microcrystalline $RbNd(MoO_4)_2$," *Journal of Crystal Growth*, vol. 318, no. 1, pp. 683–686, 2011.

[39] V. V. Atuchin, V. G. Grossman, S. V. Adichtchev, N. V. Surovtsev, T. A. Gavrilova, and B. G. Bazarov, "Structural and vibrational properties of microcrystalline $TlM(MoO_4)_2$ (M = Nd, Pr) molybdates," *Optical Materials*, vol. 34, no. 5, pp. 812–816, 2012.

[40] V. V. Atuchin, O. D. Chimitova, S. V. Adichtchev et al., "Synthesis, structural and vibrational properties of microcrystalline β-$RbSm(MoO_4)_2$," *Materials Letters*, vol. 106, pp. 26–29, 2013.

[41] L. Macalik, "Comparison of the spectroscopic and crystallographic data of Tm^{3+} in the different hosts: $KLn(MO_4)_2$ where Ln=Y,La,Lu and M=Mo,W," *Journal of Alloys and Compounds*, vol. 341, no. 1-2, pp. 226–232, 2002.

[42] L. Macalik, E. Tomaszewicz, M. Ptak, J. Hanuza, M. Berkowski, and P. Ropuszynska-Robak, "Polarized Raman and IR spectra of oriented $Cd_{0.9577}Gd_{0.0282}\square_{0.0141}MoO_4$ and $Cd_{0.9346}Dy_{0.0436}\square_{0.0218}MoO_4$ single crystals where □ denotes the cationic vacancies," *Spectrochimica Acta Part A: Molecular and Biomolecular Spectroscopy*, vol. 148, pp. 255–259, 2015.

[43] V. Dmitriev, V. Sinitsyn, R. Dilanian et al., "In situ pressure-induced solid-state amorphization in $Sm_2(MoO_4)_3$, $Eu_2(MoO_4)_3$ and $Gd_2(MoO_4)_3$ crystals: chemical decomposition scenario," *Journal of Physics and Chemistry of Solids*, vol. 64, no. 2, pp. 307–312, 2003.

[44] E. J. Baran, M. B. Vassallo, C. Cascales, and P. Porcher, "Vibrational spectra of double molybdates and tungstates of the type $Na_5Ln(XO_4)_4$," *Journal of Physics and Chemistry of Solids*, vol. 54, no. 9, pp. 1005–1008, 1993.

[45] S. S. Saleem and G. Aruldhas, "Raman and infrared spectra of lanthanum molybdate," *Journal of Solid State Chemistry*, vol. 42, no. 2, pp. 158–162, 1982.